Search for fractionally charged particles in lunar soil*

C. M. Stevens, J. P. Schiffer, and W. Chupka†
Argonne National Laboratory, Argonne, Illinois 60439
(Received 12 May 1976)

A search for stable fractionally charged particles (quarks) in lunar soil was carried out using methods based on the ionic properties which would separate quarks and distinguish them from normal elements. Previous searches in terrestrial substances are reviewed. An upper limit for the concentration in lunar soils, subject to the uncertainties in the physical and chemical properties of quarks, is 2×10^{-22}/nucleon, corresponding to a flux of cosmic-ray origin of less than 5×10^{-12}/cm^2 sec sr or 1/m^2 yr sr.

I. INTRODUCTION

The remarkable success of the quark symmetries in describing the properties of elementary particles has prompted a number of experimental searches for fractionally charged particles, both unstable and stable. Such experiments have been reviewed by Jones[1] and by Kim and Kwak.[2] Our searches for stable quarks have been carried out in various substances since 1964.[3,4]

Free and stable p-type or n-type quarks, of charge $+\frac{2}{3}e$ or $-\frac{1}{3}e$, would both result in negatively charged ionic species. Any $+\frac{2}{3}$ quarks would bind with an electron to become ions with charge $-\frac{1}{3}e$, and the $-\frac{1}{3}$ quarks would combine with positive nuclei in Bohr orbits[5] to produce atomic species with net $-\frac{1}{3}e$ charge. If a quarklike state with $-\frac{4}{3}e$ or $+\frac{5}{3}e$ were the stable one, or indeed any state with $-(n+\frac{1}{3})e$ or $+(n+\frac{2}{3})e$, they would likewise give rise to systems with net negative charge. Generally we attempted to concentrate onto small filaments negatively charged particles extracted from various substance. The negative emissions of these filaments were then studied for the presence of particles with the unusual properties quarks might be expected to exhibit: nonintegral charge resulting in dependence of volatilization on electric-field polarity, small pulse-height distribution in electron multipliers used as detectors of accelerated ions, or unusual mass peaks in mass-spectrometric analyses. The results were negative, with upper limits which were based on very uncertain assumptions regarding the physical and chemical properties of quarks both for concentrating in a particular substance and for the effectiveness of the extracting method.

In view of our ignorance, lunar material is perhaps the best place to search for such particles because of the absence of chemical and geologic metamorphism over the last eon in the top 10 meters of lunar soil. Quarks of cosmic-ray origin would tend to remain in this surface layer. In this paper, we summarize our earlier searches in terrestrial materials and present in somewhat greater detail the final results of the search made in lunar soil.

II. TERRESTRIAL MEDIA

A. Ocean sediments

Searches were made for quarks in air, dust filtered from air, sea water, and deep-ocean sediments. We have reported earlier the results on all of these[3,4] except for the deep-ocean sediments. These sediments consisted of iron-manganese nodules, which occur abundantly in the regions of the oceans far from the continental boundaries. This substance has been suggested[6,7] as a possible place where quarks might concentrate if precipitated from ocean water. In this suggestion, quarks of $+\frac{2}{3}$ charge, or quarkic oxygen or hydrogen (oxygen or hydrogen atoms with $-\frac{1}{3}$ quark bound in a Bohr-type orbit) would form quarkic water, which would be highly concentrated in the solvation shell of polyvalent positive ions and would preferentially precipitate with the hydroxide and hydrated minerals found in these sedimentation nodules. This could lead to enrichment of quarks in these minerals and much higher concentrations than in sea water, although the accumulation time is limited to the age of the minerals. At any rate, stable quarks of cosmic-ray origin would either accumulate in the water or precipitate by such a sedimentation process; a mechanism such as the "quark albedo" process proposed by McDowell and Hasted[8] is not thought to be very probable (see discussion in Appendix A).

Our search in sea water had established an upper limit of less than 3×10^{-24}/nucleon subject to the uncertainties in the assumption that quarks would volatilize from sea salt at temperatures less than 400 °C.

For the search in deep-ocean sediments, a method similar to that used for atmospheric-dust samples was used. Several hundred grams of ferromanganese mineral nodules collected at a

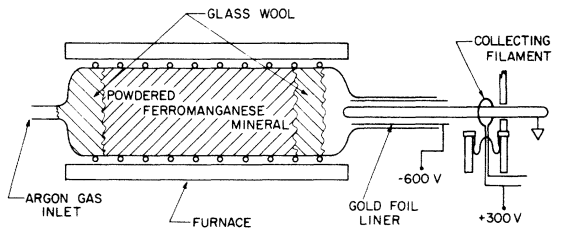

FIG. 1. Apparatus for concentrating onto a platinum filament negatively charged particles flushed from heated samples of deep-ocean ferromanganese nodules.

depth of 2000 m in the North Pacific were ground up and loaded in an oven. While the oven was heated to 800 °C, argon was flushed over the material and past a collecting filament at a positive electric potential, as shown in Fig. 1. After several hours of heating to permit any quarks of the form $H_2(Oq)^{-1/3}$,[9] $H(Hq)^{-1/3}$,[9] or $(Hq^{+2/3}O)^{-1/3}$ to diffuse out of the material, the collecting filament was mounted in the ion source of a negative-ion gun, as shown in Fig. 2. Then, using the same technique as was used in the air, dust, and seawater runs, the filament was slowly heated and the negative-ion emission was studied for any excess emission of ions above the normal background. This number was less than 10^5, corresponding to less than 10^{-21}/nucleon of sediment. Since these sediments precipitate at a rate of 3 mm/10^6 yr,[10] this limit corresponds to an equivalent ocean-water concentration of 2.5×10^{-27}

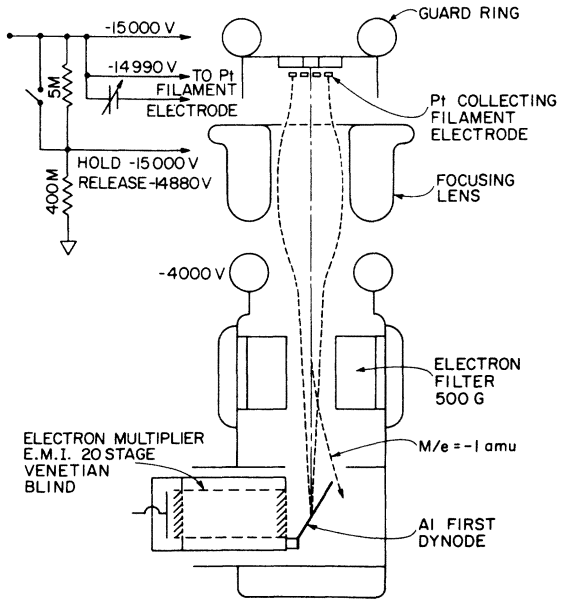

FIG. 2. Apparatus used for examining negative-ion emission of collecting filaments after the concentrating process. The dashed lines indicate ion trajectories.

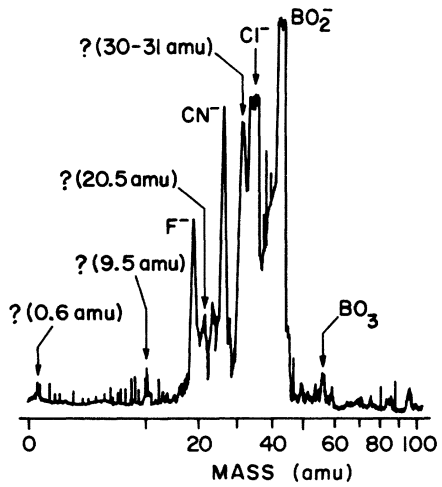

FIG. 3. Mass spectrum of negative-ion emissions of the concentrate from deep-ocean ferromanganese nodules. The filament temperature was 1000 °C.

quarks/nucleon for a 10^6-yr accumulation, assuming 100% separation efficiency.

Several runs were carried out with a Wien-filter mass spectrometer attached to the ion-gun apparatus. The apparatus was an early version of that which was used in the lunar-soil searches described below. The mass spectrum of the first run of a deep-ocean sediment separation shown in Fig. 3 exhibits several peaks of unusual masses, the atomic or molecular forms of which we have not been able to identify. The strongest of these was at mass 30–31 amu, with lesser ones at masses 20.5 ± 0.5, 9.5 ± 0.5, and ~0.6 amu. These spectra also showed peaks of several commonly observed and easily identified principal masses, such as F^-, CN^-, Cl^-, and BO_2^-, as well as minor peaks thought to be BO_2^- and BO_3^-. The peak at 31 amu, which was quite large in one instance, remains a mystery. The ion P^-, which has an electron affinity of 0.78 eV, is theoretically possible, but it should be accompanied by a much more abundant PO_2^- or PO_3^- peak, which was not the case. Likewise, any nitrogen which could produce NO^- would produce NO_2^- in greater abundance, and the latter ions were not observed. No other molecular species could account for a negative ion at 30 or 31 amu. The smaller peaks at 20.5, 9.5, and 0.6 amu are even more difficult to explain. If these peaks are due to normal elements, it is necessary to consider some unusual instrumental source, such as secondary ionization due to electrons striking an intermediate focusing electrode, or some malfunction of the Wien filter. Since these unusual peaks were only observed in the first run using a new quartz tube oven and successive runs with the same oven failed to repro-

duce them, no further efforts could be made to identify them and we ascribe them to instrumental effects.

B. High-electron-affinity ions from air and sea-water runs

In the early work on air, dust, and sea water we had observed negative ions whose emission or evaporation from the collecting filament exhibited the dependence on electric field polarity which we expected to be the unique signature of fractionally charged negative ions. A discussion of this phenomenon is given in Appendix B.

Figure 4 shows one of the runs in which the negative-ion emission exhibited this unusual signature: An exponentially decreasing intensity was retarded for a period of 20 sec by application of a retarding potential. The phenomenon was more pronounced in the air and dust runs than in the sea-water runs. Unfortunately no mass analysis was made of these ions in the air or dust runs. However, we are reasonably confident that we have identified the ions as $HP_4O_{11}^-$ (mass = 301 amu) on the basis of a mass at approximately 300 ± 3 amu observed with the Wien filter in the low-temperature emissions from one analysis of a sample separated from sea water; also, a peak with a mass of 300.9 amu was observed with the 100-inch mass spectrometer in samples prepared from the aluminum tubing used in the electric fence for the air collections, and samples of H_3PO_4 loaded directly on the filament showed an appreciable abundance of ions at a mass which measured 300.9 amu as well as an isotopic peak of mass 303 amu having an abundance about 2.2% of the 301-amu peak, as expected from the abundance of ^{18}O. In the last case the high-electron-affinity property was not present, perhaps because of different surface conditions with such a large sample. We assume that this was the species that exhibited the unusual property in all the analyses. The relative abundance of phosphorus in sea water (0.1 ppm) and in dust (estimated 0.1%)[11] is in line with the much higher intensity observed for the latter runs.

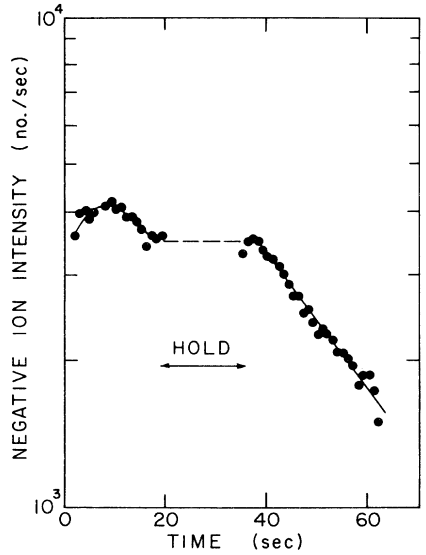

FIG. 4. Negative-ion emission vs time at 200 °C of a filament used to concentrate negative ions in air. During the interval labeled "hold" a retarding potential was applied to prevent negative-ion emission from the filament.

If, on the other hand, these ions were quarks, their relative abundance in air (10^{-30}/nucleon), dust (2×10^{-28}/nucleon of equivalent air), and sea water (3×10^{-24}/nucleon) does not fit our estimate of relative concentrations; the value for the atmosphere is much too large compared to that for sea water or to the value based on direct cosmic-ray searches.[1]

III. LUNAR MATERIAL

Initial measurements were carried out with small samples (fractions of grams) obtained from the Apollo 11 and 12 lunar missions. These were heated in a crucible mounted in the ion source of the 100-inch mass spectrometer and the mass spectrum from 16 to 80 amu was examined for any unusual masses. The results were negative. The limits that can be set are not very low because of the low efficiency inherent in scanning a wide mass range and the presence of many integral mass peaks from the normal elements. To overcome these difficulties, we utilized an improved experimental arrangement similar to that employed during the earlier work for air and sea-water samples. Several grams of lunar soil were heated slowly in a crucible up to the melting point of the soil. This crucible was the source for an ion gun and all the negative ions emitted were implanted in a clean rhenium filament. The subsequent negative-ion emissions of these filaments were then studied for any possible quarklike properties. This process should have reduced by many orders of magnitude the number of reemitted impurity ions such as O^-, Cl^-, and S^- relative to quarklike material, because of the low surface ionization efficiency for negative ions of all the known elements.

A. Apparatus

The experiment is illustrated schematically in Fig. 5. It consisted of an ion source with an accelerating electrode system, a crossed-field Wien mass analyzer, and a target system consisting of either a Faraday cup for mounting the implantation

filament or an electron multiplier located 0.0125 rad off the beam axis. This apparatus was used for both steps of the procedure: the implantation in a rhenium filament, and the examination of the negative ions which were reemitted from this target filament. For the latter step, the filament was moved from the target position and mounted in the ion source in place of the crucible.

The focusing properties of the ion source with the einzel lens located at the exit of the analyzer resulted in nearly 100% transmission of the 15-kV ion beam, from either the 1.5-mm-diameter orifice of the crucible or the 1.25 mm×3 mm target filament, to a 2 mm×3 mm collector slit. The ion beam was aligned by radial and "z" deflection electrodes located at the exit of the ion source and the entrance of the analyzer.

The crossed-field analyzer was operated with zero resolution for the most part, i.e., for more than 90% of the time during the implantation runs and for all the measurement of the emissions from the target filament after implantation. The crossed field was used occasionally during the crucible runs to examine the mass distribution of the ion beam at various temperatures. It was also useful in calibrating the pulse-height distribution of the electron multiplier for various masses. In order to have truly zero resolution, it was necessary to cancel the residual magnetic field of the analyzer by means of a small current through the coils of the electromagnet. The electron multiplier detector was an EMI 20-stage "venetian-blind" unit with a polished aluminum first stage at a 45° angle to the ion beam axis.

The square-wave 60-Hz voltage, with adjustable duty cycle, could be applied to the radial deflection plates at the exit of the crossed-field analyzer in order to carry out two-stage implantation. Using this feature, 50% of the ions reemitted from one implantation-target filament could be implanted in a second target filament, while the other 50% was monitored by the electron multiplier. This feature was used in some of the runs.

Several materials were tried for the target filament. Zone-refined rhenium was chosen for a number of reasons: low background negative-ion emission, high work function, and low vapor pressure at the temperatures used to bake out impurity contamination. Two matched filaments were used for all the implantations (except run A as shown in Table I). These filaments were 0.025 mm×1.25 mm zone-refined rhenium ribbon shaped as a hairpin with a 3-mm-long flat section as the target area. The filament for run A was the same except that it was 0.05 mm×0.75 mm in cross section. The filaments were mounted at the target end inside a Faraday cup with the filament insulated at −45 V with respect to the cup so that the collection of the ions on the filament could be monitored whenever possible by a vibrating-reed electrometer. When the ion current was too low to be detected directly by this method, the beam was deflected to the electron multiplier using the beam-deflection facility with a 10–15% duty cycle.

The system was pumped by a turbomolecular pump and a 5-in.-diameter liquid-N_2 trap located above the ion source; the latter had a very high pumping speed for condensables both during the heating of the lunar samples and during that of the target filament. A 4-in. valve was located between the ion source and rest of the system to minimize the exposure to air during the extensive preliminary tests.

B. Negative-ion emission from lunar samples heated in a crucible

The lunar-soil samples were loaded into a platinum crucible 1.0 cm in diameter and 4.5 cm long with a 1.5-mm orifice. The crucible was inside an alumina cylinder around which was wound the platinum heating wire, with the crucible itself

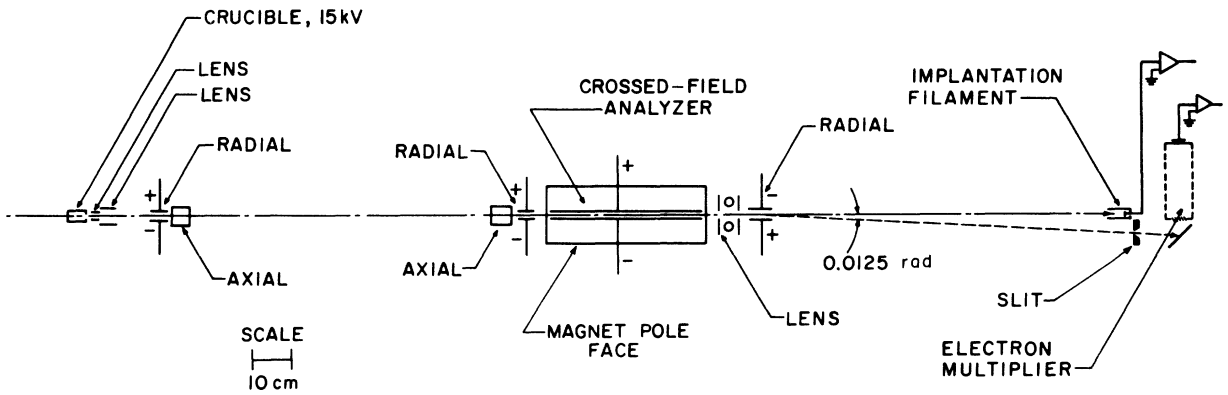

FIG. 5. Apparatus used both for concentrating onto rhenium target filaments the negative ions emitted from heated lunar soil samples and also for examining the negative-ion emissions of these target filaments.

TABLE I. Summary of implantation runs of negative ions onto rhenium target filaments from heated samples of lunar soil.

Run no.	Amount of lunar soil (g)	Remarks
A	0.25	Two-stage implantation of emissions from gold foil in which all negative ions from lunar soil had been implanted
B	2.2 [a] +2.6	Implantation from lunar soil onto target filament
C-1	0.4 [a] +4.0 [a] +3.0	Implantation from lunar soil onto target filament
C-2		Implantation of 50% of negative ions from run *C*-1
D-1	3.0	Implantation from lunar soil onto target filament
D-2		Implantation of 50% of negative ions from run *D*-1

[a] Incomplete implantation because of instrumental difficulties and adjustments in focusing.

TABLE II. Mass spectra of negative ions from 3.0 g of lunar soil sample 10084.17. See Fig. 6 for the time and temperatures corresponding to spectrum numbers.

Mass (amu)	Probable atomic or molecular species	Relative intensity of mass peak in % of total intensity Spectrum 1	2	3	4	5	6
12	C^-			0.2			
16	O^-		13	7	19	5	18
19	F^-		7	13	19	5	15
24	C_2^-		20	32			
25	C_2H^-		13	1			
26	CN^-		20	23	1	1	4
27	$C_2H_3^-$		4	1	2		9
32	O_2^- and S^-		7	9	45	15	3
35	$^{35}Cl^-$		1.4	5	3	4.5	0.7
36	C_3^-			0.8			
37	$^{37}Cl^-$		0.5	2	1		0.2
42	$^{10}BO_2^-$		2	0.4	2	7	3
43	$^{11}BO_2^-$		11	1.6	8	28	13
48	SO^-			3			
50	?			0.9			
59	?					4	
64	SO_2^- (?)	4			2	32	12
72–80	PO_3^- (?)	7					10
85–90	?						0.1
90–96	?						0.6
300 ± 10	$HP_4O_{11}^-$ (?)	15					
2500 ± 300	?	73					
Total ion intensity (A)		2×10^{-17}	7×10^{-15}	10^{-12}	5×10^{-12}	3×10^{-11}	10^{-10}

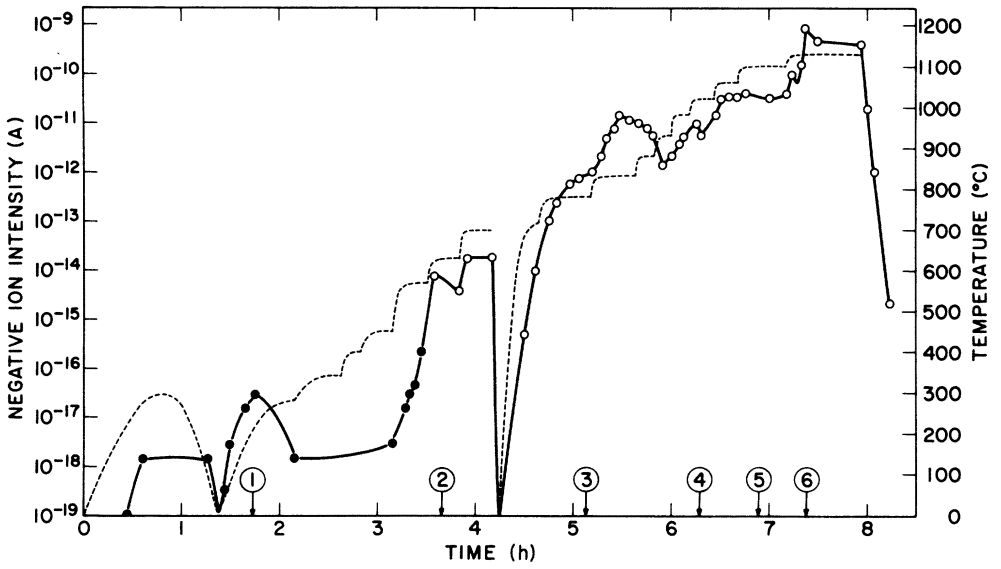

FIG. 6. Negative-ion intensity (solid line) and temperature (dashed line) versus time during the heating of 3 g of lunar soil sample No. 10084.17. The numbers on the time axis indicate times at which the mass spectra of Table II were taken.

providing one of the leads to the heating element. The alumina cylinder also provided the insulation between the extraction electrode and the crucible. Electrical leakage always occurred between the crucible and the extraction electrode after the loaded crucible was installed in the ion source and the system was evacuated and until the crucible was heated slightly. The leakage was probably due to surface adsorption of water on the alumina. During the time the leakage occurred there was a small negative-ion emission, which seemed to come from a broad source such as the whole front face rather than the orifice of the crucible. The apparent mass of these ions was very high, 1000–2500 amu.

The lunar samples were heated stepwise at a rate such that the pressure at no stage exceeded 6×10^{-7} Torr. The maximum temperature was in the range 1100–1200 °C and corresponded to partial melting of the soil.

Table I lists the implantation runs and corresponding amounts of lunar samples. Figure 6 shows the total ion intensity and the temperature versus time for the ion emission from one of the crucible loadings, and Table II gives the mass distribution of the ions emitted from the crucible at several temperatures of the heating cycle indicated in Fig. 6.

C. Background emission of target filaments

Table III lists eight background runs with the target filaments after they were baked out in a vacuum and then exposed to room air for various lengths of time from 15 min to 4 days. This was done in order to duplicate the effects of any contamination which might have been introduced during the transfer of the filament from the target to the ion source. Figure 7 shows the ion intensities for these background runs versus filament current and temperature. The number of negative ions emitted during a 30-sec period after the filament current was set at the indicated value is plotted. The background emissions are characterized by three fairly distinct regions:

(1) a low-temperature region, 100–240 °C, in which there were about 20–100 ions emitted with a rapidly decreasing rate ($T_{1/2}=10$ sec),

(2) a region between 260 and 600 °C in which there were less than ten detectable negative ions,

(3) a region above 600 °C in which negative-ion emission always occurred, was fairly constant at any one temperature, and increased as the temperature was increased.

The emission in the low-temperature region is very likely due to surface-adsorbed impurities such as aerosols which deposited on the filament

TABLE III. Background runs of negative-ion emissions of rhenium filament exposed to air.

Run no.	Exposure time to air
1	3–4 days
2	20 minutes
3	1 hour
4	1 hour
5	20 minutes
6	30 minutes
7	20 minutes
8	15 minutes

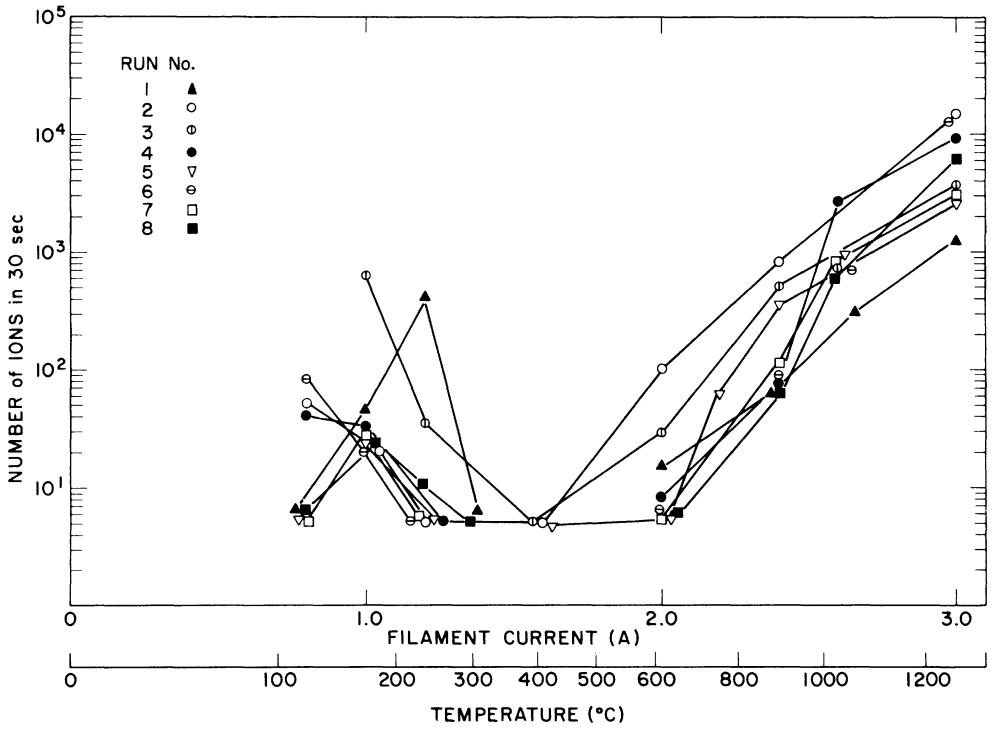

FIG. 7. Negative-ion intensity versus filament current (and temperature) of background runs on rhenium filaments.

during the exposure to air and were rapidly desorbed even at these relatively low temperatures. These impurity ions were all volatilized below 240 °C even in the runs having the most contamination. We have discussed earlier a negative ion species, $HP_4O_{11}^-$, which is produced at temperatures unusually low for negative-ion formation and hence must have very high electron affinity. This may account for the low-temperature background ions.

No background negative ions were observed between 250 °C and 600 °C. The ion emission above 600 °C was for the most part constant with time and increased exponentially with temperature. These ions, which were identified as O^-, F^-, and Cl^-, probably originated from background gas impurities in the vacuum system. Taking the Saha-Langmuir ionization for Cl^- from a rhenium surface at 600 °C as 10^{-4}, the corresponding partial pressure of the chlorine containing impurity must have been about 10^{-16} Torr. Some of this background was undoubtedly due to the release of gases from the warming of components adjacent to the filament.

The negative-ion emission varied more than an order of magnitude in both the low- and high-temperature regions. The emission in the low-temperature region was proportional to the time of exposure to air, whereas in the high-temperature region there was no correlation with the amount of exposure to air.

D. Emissions of target filament after implantation

The negative-ion emission of the target filaments following implantation is shown in Fig. 8. Compared to the background runs, the number of ions emitted was significantly greater in the temperature range 200–320 °C, and essentially the same at all other temperatures. The excess began at a slightly lower temperature than that for the maximum of the background runs in this range. That these excess emissions in the implantation runs were of different origin then the background emissions is shown by their rate of decay; the decay rate for the implantation run, shown in Fig. 9, was much slower than those for the background runs, shown in Fig. 10. The number of these excess ions corrected for the losses from beam splitting, where used, were 335 ± 10 for run *B*, 70 ± 10 for run *C*-1, 90 ± 40 for run *C*-2, and 60 ± 20 for run *D*-1. The results of the other runs and the probable cause of the variability in all the runs are discussed in Appendix C.

The excess ions emitted in the implantation runs were too few to permit identification with the Wien-filter mass spectrometer. However, we attempted to learn some of the characteristics of these ions from the diffusion properties for the

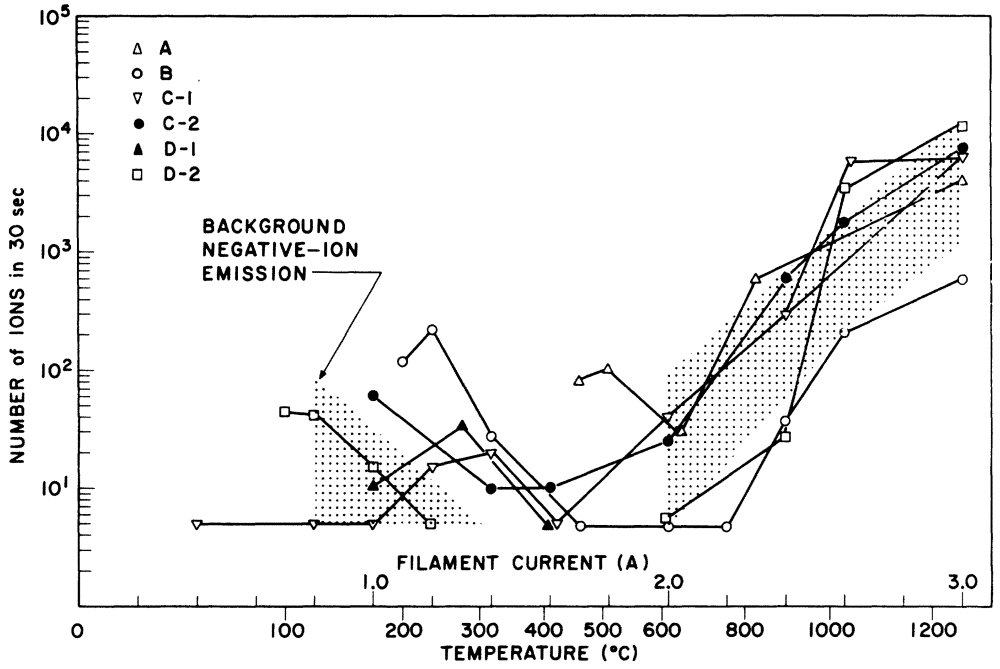

FIG. 8. Negative-ion intensity versus filament current (and temperature) of rhenium target filaments after implantation of negative ions emitted from heated lunar samples. The shaded area represents the range of background intensities.

implanted ions and their pulse-height distribution from the electron multiplier detector.

We show in Appendix D that the diffusion coefficient of the excess ions emitted in the implantation runs is similar to that of the electronegative elements which produce negative ions most abundantly, such as the halogens, oxygen, sulfur, and nitrogen (CN^-). Thus, it is reasonable to expect that after implantation of $\sim 10^{12}$ atoms of chlorine in the target filament, 10^2–10^3 negative ions of chlorine may be reemitted from the filament at 200 °C.

The pulse-height distribution of an electron multiplier depends on the mass, kinetic energy, and molecular form of the impinging ion.[12] Figures 11 and 12 show the characteristic pulse-height distributions for the electron multiplier used in this experiment. Unfortunately such data were obtained for only a small number of emitted ions in one of the implantation runs, *D*-1, shown in Fig. 13, and while the result was similar to the distribution for Cl^- ions at one-third the accelerating potential, it was also close to that for $HP_4O_{11}^-$, and to the low-temperature emissions of the background runs.

This meager amount of data suggests that the excess ions observed in the implantation runs were due to the initial implantation of an abundant species such as PO_3^- in the emissions from the lunar soil, followed by diffusion of these implanted phosphorus atoms to the surface, where they combined with absorbed H_2O to form some volatile high-molecular-weight species such as $HP_4O_{11}^-$ with a relatively high electron affinity.

Implantation run *B* was the most successful, showing a maximum of 335 excess ions reemitted

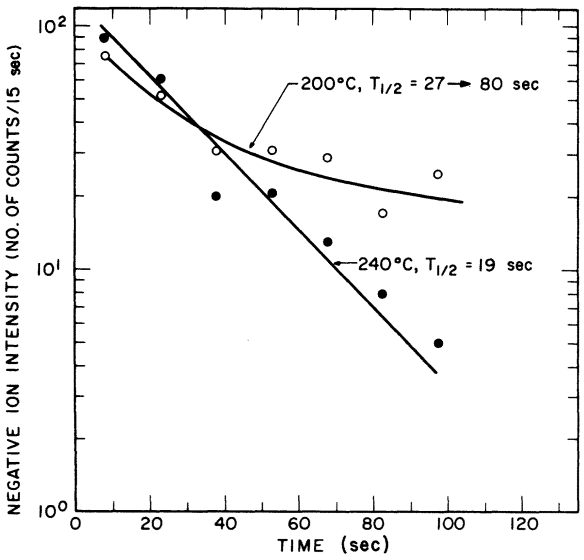

FIG. 9. Intensity versus time, after reaching a given temperature for the first time, of emissions from implantation run *B* at temperatures of 200 and 240 °C.

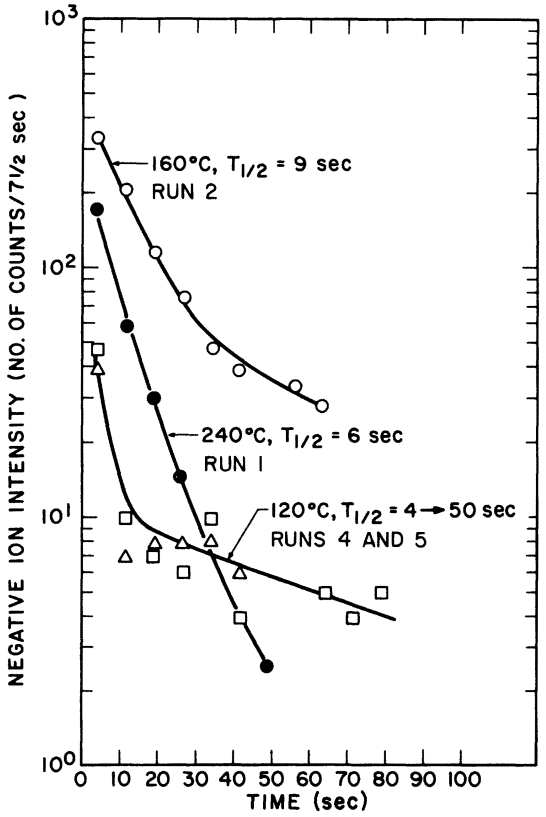

FIG. 10. Intensity versus time, after reaching a given temperature for the first time, of background emission from rhenium filaments at temperatures of 120, 160, and 240°C.

below 600 °C. The emissions above 600 °C in this run were as low as the lowest-level background runs, amounting at 1000 °C to 250 ions, undoubtedly Cl^-. We conclude that the upper limit for

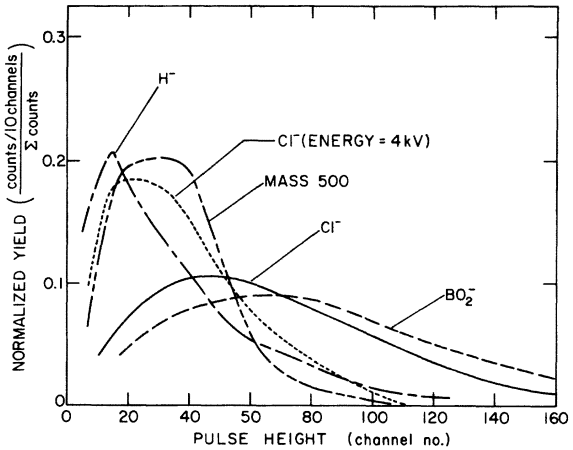

FIG. 11. Pulse-height distribution of H^-, Cl^-, BO_2^-, and an unidentified peak at about 500 amu in the electron multiplier detector. The ion energy at the first dynode of electron multiplier was 12 kV except as noted.

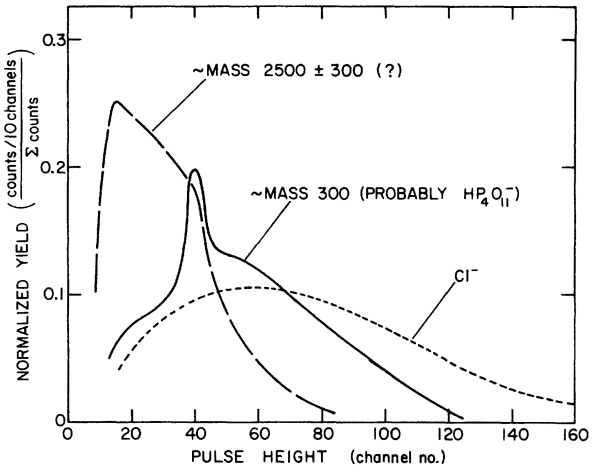

FIG. 12. Pulse-height distribution of Cl^-, $HP_4O_{11}^-$, and an unidentified peak at about 2500 amu with ion energy of 12 kV.

quarks in the lunar-soil sample 10 084 is less than 130 g^{-1} or less than 2×10^{-22}/nucleon.

IV. DISCUSSION

Table IV gives a summary of all our searches, showing the limiting concentration per nucleon, ρ, and the corresponding limiting flux for a cosmic-ray origin, $\phi \equiv \rho N d/2\pi T$. Here N is 6×10^{23} nucleons/g, d is the effective thickness of the medium in g/cm^2, and T is the accumulation time in seconds. For lunar soil the effective thickness from the probable range of cosmic-ray quarks, or quarks produced by cosmic-ray primaries, is estimated at 3 kg/cm^2; this is a depth of ~10 m, and is greater than the mixing depth from the "gardening" action on lunar soil. For the Apollo 11 sample used in this work (No. 10 084) we take the value of 300×10^6 yr as the cosmic-ray-exposure age, based on measurements of spallation-

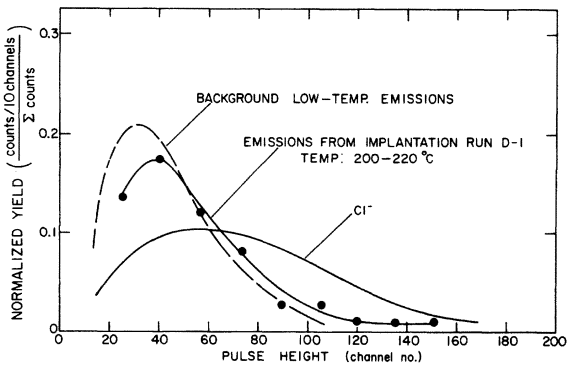

FIG. 13. Pulse-height distribution of the low-temperature negative-ion emissions from a background run and the emissions at 200–200°C of implantation run D-1 with ion energy 12 kV.

TABLE IV. Summary of limiting quark concentration and cosmic-ray fluxes.

Medium	Upper limit of concentration (no./nucleon)	Effective thickness of medium (g/cm^2)	Accumulation time (sec)	Upper limit of flux (no./cm^2 sec sr)
Air	10^{-30}	10^3 [a]	10^6 [a]	10^{-10}
Dust	2×10^{-20} [b]	10^3 [a]	10^6 [a]	2×10^{-8}
Sea H_2O	3×10^{-24}	3×10^5 [c]	10^{17} [d]	1×10^{-12}
Deep-ocean sediment	10^{-21}	0.75 [e]	3×10^{13}	3×10^{-12}
Meteorite	10^{-17}	3×10^3 [f]	1.0×10^{16} [g]	3×10^{-7}
Lunar soil	2×10^{-22}	3×10^3 [f]	1.0×10^{16} [g]	5×10^{-12}

[a] Based on standard atmosphere and residence time of 10 days.
[b] Concentration in equivalent amount of air is 2×10^{-28}/nucleon.
[c] Average depth of ocean is 3000 m.
[d] Assume galactic cosmic-ray exposure age as long as age of oceans.
[e] Based on accumulation rate of 3 mm/10^6 yr of ferromanganese nodules (density = 2.5 $g\,cm^{-1}$).
[f] Assumed maximum range of galactic cosmic-ray primaries.
[g] Assume galactic cosmic-ray exposure age of 3×10^8 yr.

induced rare-gas isotopes.[13] We have discussed in our previous paper the uncertainties in the extraction efficiencies for the air, dust, and sea-water separations. We consider the result for lunar soil to be the least doubtful. Certainly the extraction was far superior in the lunar case to that for the others because of the much higher temperature (~1100 °C) at which the extraction process was carried out.

It is possible that quarks might have properties which would have resulted in their being lost during or after the collection process. If, as seems chemically unlikely, quarks were highly volatile and had fast hydrogenlike diffusion rates, they may have been lost between the time the implantations were carried out and the time the target filament was examined, or they may even have been lost from the topmost layers of the lunar surface. There is evidence for depletion on the lunar surface of Hg, Br, and Ar because of such processes.[14,15]

During the course of this series of studies, several phenomena were observed which might concievably have been due to quarks. These were the ions with unusually high electron affinity observed from air, dust, and sea water, the unusual masses in one run of the deep-ocean sediments, and the excess ions emitted in the lunar implantation runs. We are reasonably satisfied that all these phenomena were caused by some property of normal elements or compounds. The limits in Table IV were in all cases based on including these unusual phenomena as the upper limit of quark concentration. If these ions were attributed to some species of the normal elements, as we have attempted to demonstrate, then in the cases of both the sea-water experiments and the lunar-soil experiments the limiting concentrations would be an order of magnitude lower than the values quoted in Table IV.

V. SUMMARY

Of all the materials available, the lunar-surface soil is the best medium in which to search for quarks from cosmic radiation. The limiting flux is 5×10^{-12} cm^{-2} sec^{-1} sr^{-1} ($1\ m^{-2}\ yr^{-1}\ sr^{-1}$), at least an order of magnitude lower than direct cosmic-ray counting experiments, and applies to $-\frac{1}{3}e$ and any $+(n+\frac{2}{3})e$ or $-(n+\frac{1}{3})e$ quarks. Most of the uncertainty caused by chemical and geological variables in previous quark searches in stable matter is removed because of the stability of the lunar surface. This flux may be interpreted as a production cross section for $-\frac{1}{3}e$ or $+\frac{2}{3}e$ quarks by high-energy cosmic-ray primaries, as a function of quark mass; the relationship is somewhat model-dependent and is not carried through here.[1,16]

ACKNOWLEDGMENTS

We are indebted to Ed Goldberg and Tom Walsh of the Department of Earth Sciences, University of California, San Diego, California for kindly supplying us with ferromanganese mineral samples. Also, we gratefully acknowledge Steve Rothman, John Reynolds, P. Pepin, and M. Anbar for helpful discussions. The electronics design and maintenance were carried out by Robert Lewis and Larry Van Loon.

APPENDIX A

The suggestion by McDowell and Hasted[8] was that during the recycling of water between atmosphere and ocean the quarkic oxygen and hydrogen species would eventually be separated by the atmospheric electric field and drift up to the mesosphere. We think it is not very likely that any quarks (either + or −) bound to H_2O will be readily lost from sea water by this process. The vapor pressure (evaporation rate) for such charged molecular species will be much lower than that of ordinary H_2O. The estimated extra heat of solvation of such an ion with $\frac{1}{3}$ charge would be at least 10 kcal/mol [by use of the Born equation $\Delta H = e^2(1 - 1/D)/2r$, with dielectric constant $D \gg 1$, and comparison with other ions]. This would result in a vapor pressure decrease (compared to H_2O) of $\exp(-H/kT)$, which is about 10^{-6} at 300 °K and it is more likely to be of the order of 10^{-9}. Species of charge $\frac{2}{3}$ would be still very much less volatile. Therefore, since the average residence time of all ocean water is 10^9 years, it seems very likely that the loss rate from the ocean by evaporation would be less than $10^{-9}\ n$/year, where n is the average ocean-water concentration.

APPENDIX B

The rate of volatilization of negative ions from a metal surface compared to that for the neutral species depends, in analogy with the Saha-Langmuir relation, or $\exp[-1(W - A)/kT]$, where W is the work function of the surface and A is the electron affinity of the ion. The volatilization rate of the neutral species is expected to be many orders of magnitude greater than that for negative ions. This is certainly the case for all of the simple atomic or diatomic species with highest electron affinities (3.0–3.5 eV for F^-, Cl^-, CN^-) volatilizing from a platinum surface ($W \sim 5.0$ eV) used in this work. Thus, if a retarding potential were applied to the filament during a time when the intensity of negative-ion emission is decaying, indicating a decreasing concentration of the species on the surface, the volatilization rate would not be appreciably affected and the concentration would continue to decrease. After the retarding potential is removed, the negative-ion intensity should resume at the reduced value of the extrapolated decreasing intensity. Fractionally charged negative ions, on the other hand, since they cannot form the neutral species, could not evaporate when the retarding electric field was applied, and assuming they are not lost as positive ions by combining with some element such as sodium, they would be reemitted at an intensity equal to the value existing when the retarding potential was applied. For any ions made up of the normal elements to exhibit this characteristic, such as shown in Fig. 4, then, from the standpoint of Saha-Langmuir ionization, the electron affinity of these ions would have to be very high, >5 eV, for emission from a platinum surface. Recently, electron affinities of 4 to 5.4 eV have been reported for several hexafluoride molecules.[17] Another possibility is that the work function of the surface was lowered by adsorbed impurities.

APPENDIX C

The results of run A were peculiar. This was a run after two stages of implantation starting with a 0.25-g sample of lunar soil. The first implantation was made in a gold foil target; then this foil was heated up in a crucible and the emissions from it were implanted in a rhenium filament. No emissions were observed from the rhenium filament at temperatures under 450 °C, perhaps because of poor beam alignment, yet there were appreciable emissions in the temperature range of 450–500 °C which did not occur on any other run. We do not know whether these ions were due to accidental contamination or possibly to some gold compound of high electron affinity. We do not attach any significance to this result, as the sample size was small and these emissions did not show up in any of the other one-stage implantation runs on large samples. Run D-2, after two stages of implantation, showed an ambiguous result of 99 counts at

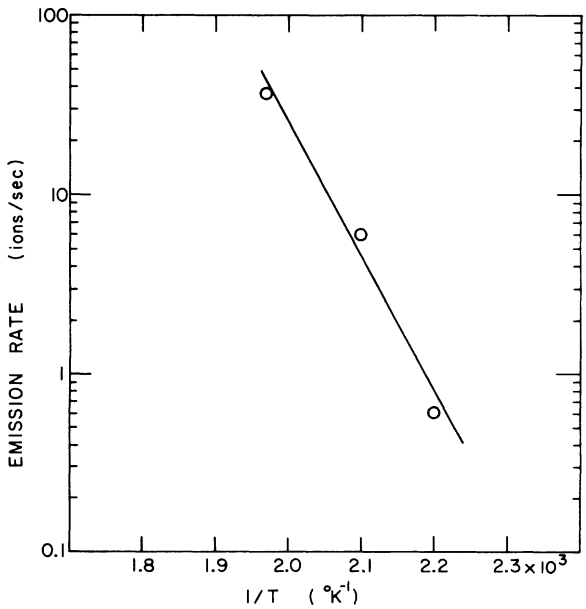

FIG. 14. Initial intensity of emissions from run B versus $1/T$.

120 °C. While this number is within the range of values for the background emissions at this temperature, the rate of decay was slower than that for the usual background emissions at the same temperature.

The poor reproducibility of the runs was probably the result of the difficulty in aligning the beam after installing the target filament in the ion source. Although great care was taken to establish the correct settings for the several beam deflection and focusing voltages using duplicate filament mountings, and these voltages were varied during the heating of the filament, there was no other way to assume that the alignment was correct for the initial very-low-intensity emissions. Once emissions of a few counts per second were detected, it was possible to quickly adjust the settings to maximum intensity. In retrospect, the ion optics design was too sensitive to the filament position, because it was designed for moderately high mass resolution of the Wien-filter mass spectrometer, a feature that did not turn out to be important.

APPENDIX D

For the one-dimensional form of the diffusion equation,

$$\frac{dN}{dt} = -DA\frac{\partial C}{\partial x},$$

$$\frac{d(dN/N)}{dt} \sim -\frac{D}{x^2},$$

where N is the number of ions implanted to a depth of x cm in a filament of area A cm^2. Since typical implantation depths for 15-kV ions are of the order of 100 Å, the diffusion coefficient corresponding to the initial decay rate of 2.6%/sec at 200 °C, corresponding to the intensity in implantation run B shown in Fig. 9, would be less than 10^{-14} cm^2/sec. This rate of diffusion, for interstitial diffusion with $D \sim \frac{1}{10}e^{-Q/kT}$, corresponds to an activation energy greater than 33 kcal/mol. The temperature dependence of the decay rate for run B, shown by the Arrhenius plot in Fig. 14, gives an activation energy of 35 kcal/mol. There are few measured activation energies for diffusion in rhenium of the electronegative gases such as the halogens, O, S, and N(CN^-). Because rhenium has a hexagonal close-packed lattice and a high melting point, the diffusion of such gases would be expected to be quite slow, corresponding to activation energies greater than 30 kcal/mol. For nitrogen diffusion in rhenium at low temperatures, $Q = 37$ kcal/mol.[18] Free quarks of the form $+\frac{2}{3}e$, on the other hand, would be expected to diffuse many orders of magnitude faster, at values similar to hydrogen or alkali ions. Thus, the slow diffusion rate of the excess ion emissions of the implantation runs suggests an atomic species such as N, O, S, or Cl.

---

*Work supported in part by NASA under Contract No. T90267 and in part by U. S. Energy Research and Development Administration.

†Present address: Department of Chemistry, Yale University, New Haven, Conn. 06520.

[1]W. J. Jones, Phys. Today 26, No. 5, 30 (1973).

[2]Y. S. Kim and N. Kwak, Fields and Quanta 3, 1 (1972).

[3]W. A. Chupka, J. P. Schiffer, and C. M. Stevens, Phys. Rev. Lett. 17, 60 (1966).

[4]C. M. Stevens, J. P. Schiffer, and W. A. Chupka, in *Proceedings of the Second Lunar Science Conference*, edited by A. A. Levinson (MIT Press, Cambridge, Mass., 1971) [Geochim. Cosmochim. Acta Suppl. 2 (1971)], Vol. 3, p. 2671.

[5]Whether there is attractive or repulsive strong nucleus-quark interaction is irrelevant for this purpose, as is the question of the stability of a quarkic nucleus against β decay. The final nucleus will always have a charge of $(Z - \frac{1}{3})e$, and will generally bind Z electrons; thus most of the atoms will have $-\frac{1}{3}e$ charge.

[6]M. Anbar, personal communication.

[7]A. Nir, Phys. Rev. Lett. 19, 336 (1967).

[8]M. R. C. McDowell and J. B. Hasted, Nature 214, 235 (1967).

[9]The bracket denotes a $q^{-1/3}$ quark captured by an oxygen or hydrogen nucleus.

[10]M. L. Bender, Teh-Lung Ku, and W. S. Broecker, Science 151, 325 (1966).

[11]R. Johansson, R. Akelsson, and S. A. E. Johansson, Nucl. Instrum. Methods 84, 141 (1970).

[12]M. G. Inghram and R. J. Hayden, *A Handbook of Mass Spectrometry*, National Research Council Nuclear Science Series No. 14 (1954).

[13]C. M. Hohnenberg, P. K. Davis, W. A. Kaiser, R. S. Lewis, and J. H. Reynolds, in *Proceedings of the Apollo 11 Lunar Science Conference, Houston, 1970*, edited by A. A. Levinson (Pergamon, New York, 1970) [Geochim. Cosmochim. Acta Suppl. 1], Vol. 2, p. 1283.

[14]G. Reed and S. Jovanovic, in *Proceedings of the Second Lunar Science Conference* (Ref. 4), Vol. 2, p. 1261.

[15]R. H. Manka and F. C. Michel, in *Proceedings of the Second Lunar Science Conference* (Ref. 4), Vol. 2, p. 1717.

[16]Robert K. Adair and Nancy J. Price, Phys. Rev. 142, 844 (1965).

[17]C. D. Cooper, R. N. Compton, and P. W. Reinhardt, in *Electronic and Atomic Collisions: Abstracts of Papers of the IXth International Conference on the Physics of Electronic and Atomic Collisions*, edited by John S. Risley and Ronald Geballe (University of Washington Press, Seattle, 1975).

[18]John Askill, *Tracer Diffusion Data from Metals, Alloys and Simple Oxides* (IFI/Plenum, New York, 1970).